

6G OTA Measurements at Sub-THz Band Using a Compact Robotic System

Asad Husein, Kimmo Rasilainen, Juha-Pekka Mäkelä, Aarno Pärssinen, and Marko E. Leinonen
 Centre for Wireless Communications, University of Oulu, Finland
 asad.husein@oulu.fi

Abstract—As development in the sub-THz band (100-300 GHz) for antenna designs, specifically towards radio systems for potential sixth generation (6G) wireless communications is progressing, accurate characterisation of these complex antennas requires more sophisticated measurement setups. Robotic scanning systems have ushered in configurability to the measurement setups; however industrial sized robots cannot be accommodated in a lab environment for R&D measurements. Compact robots will be required to conduct over-the-air (OTA) performance measurements for 6G radios, and this work presents the development of such a system to cater for upcoming academic and industrial needs. Initially, the system has been characterised to perform sub-THz far-field (FF) OTA measurements. The E- and H-plane copolar patterns are determined using the measurement setup and compared to electromagnetic (EM) and planar near-field (NF) measurements illustrating good matching of the main and side lobes at 110-170 GHz band, thereby validating the performance of the developed robotic measurement system.

Index Terms—antennas, robot based antenna measurements, far-field pattern, sub-THz, 6G.

I. INTRODUCTION

There is an increasing exploration by academia and industry in antenna designs at the sub-THz band (e.g., 100-300 GHz) for future sixth generation (6G) extreme data rate wireless communication systems due to large available bandwidth [1]. The need to accurately measure the radiation characteristics of such sophisticated antenna designs using a reliable measurement setup in the sub-THz band has become indispensable. Radiated measurements can consist of either performing near-field (NF) measurements or far-field measurements (FF) which are carried out over-the-air (OTA). The FF region or commonly referred to as the Fraunhofer region of an electrically large antenna is defined as $2D^2/\lambda$, where D is the largest antenna dimension and λ is the wavelength of the antenna [2]. The FF region for antennas of different sizes and/or frequencies varies whether it is for a single-element or array antennas. In recent years, NF measurements are being preferred for certain scenarios as they provide the affordability to operate in electromagnetic-shielded environments and handle the challenges presented from FF measurements [3]. The existing measurement systems thereby incorporate the ability to either perform FF or NF measurements limited in the geometries of their movement and flexibility in measuring distances and frequency ranges. A unique approach to antenna measurements was proposed by NIST [4] to utilise industrial sized robotics for reconfigurability between NF and FF measurements within the same measurement system. The idea of using robotics

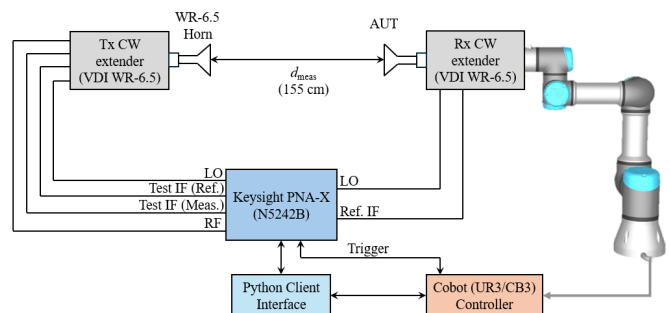


Fig. 1. Block diagram of measurement setup at University of Oulu.

supported antenna measurements has been investigated in different setups and case scenarios, for instance in [5]–[8].

This paper presents the development of a similar antenna measurement system at the University of Oulu based on collaborative robots (cobots) which can safely function around people without the need of safety infrastructure that industrial robots commonly require. Experimental results obtained thereby validate the characterisation of the measurement system. In the next stage we plan to extend its capabilities to perform NF measurements at different trajectory geometries.

II. COBOT SYSTEM

The cobot measurement system at the University of Oulu is currently located in the anechoic chamber. A block diagram of the measurement setup has been depicted in Fig. 1. It primarily consists of a cobot arm, a performance network analyzer (PNA-X) N5242B from Keysight Inc. and an external computer that communicates with the cobot arm using real time data exchange (RTDE) over TCP/IP protocol.

A. Cobot Arm

A compact UR3/CB3 model from Universal Robots has been employed in the measurement setup. It is a table-top cobot having a reach of 500 mm and a payload capacity of 3 kg. The cobot is based on a serial kinematic model with 6 rotating joints that can provide linear and angular scanning at a positional repeatability of $\pm 100 \mu\text{m}$. At this stage of developing the measurement system, the cobot is mounted on a mobile workbench. Future plans include to develop a more stable and tractable basis to make the cobot more portable and to further reinforce the stability of the measurement setup by way of handling the vibrations from the joint motor backlash.

Owing to its small size it can be easily integrated with other radio frequency (RF) measurement systems, especially those dealing at sub-THz frequencies for instance probe station based measurements, reconfigurable intelligent surface (RIS) measurement systems where the devices under test would be considerably compact.

B. Trajectory Planning

The initial measurement trajectory that has been considered is an azimuth sweep spanning from $\pm 60^\circ$ at a step size of 1° , but the range could be extended to a $\pm 150^\circ$ azimuth range in the current configuration of the measurement system. The azimuth sweep has been performed only at a single elevation angle making the measured data points less dense than in traditional FF measurements. A simulation of the measurement trajectory was visualised in RoboDK software wherein you can import the UR3/CB3 model from their available libraries. The model was further appended with a payload design of the receiving module which consists of a receiving frequency extender and horn antenna to the Tool Center Point (TCP) flange on the sixth joint (Wrist3) of the cobot. The visualisations rendered in the RoboDK software helped us in understanding the inverse kinematics and motion of the cobot arm in the joint and Cartesian space. A planar trajectory has also been developed with a grid size of 35 cm x 30 cm and plans include to use this in NF based measurements to extend the configurability of the cobot measurement system. There are also other trajectories in development for studying non-canonical approaches to measurements catering the need for future systems.

C. Software Control System

A real-time data exchange (RTDE) protocol over a standard TCP/IP connection was utilized to interact with the fieldbus drivers of the UR controller in order to manipulate the cobot I/O and plotting status which in essence are different cobot trajectories. Once the RTDE interface connection has been established, any combination of the input and output registers that the client would need to write and read within the cobot controller may be specified. In order to achieve this, the client will send a setup list of named input and output fields contained in a data synchronization package format commonly referred to as a recipe. A list of the field names and its associated types along with its functionality has been provided on the UR support website. In this measurement setup a Python based software client was implemented where the translation and rotational pose coordinates of the $\pm 60^\circ$ azimuth range was defined. The pose coordinate values were extracted from the UR controller itself by running an independently designed program of this trajectory in the polscope graphical user interface of the cobot.

III. RF MEASUREMENT SYSTEM OVERVIEW

A. Hardware Instrumentation

A four port 26.5 GHz PNA-X was used together with WR6.5 band (110-170 GHz) continuous wave (CW) frequency

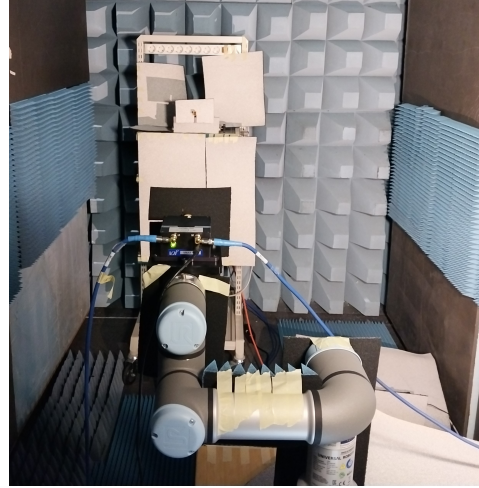


Fig. 2. Photo of the cobot measurement setup in the anechoic chamber.

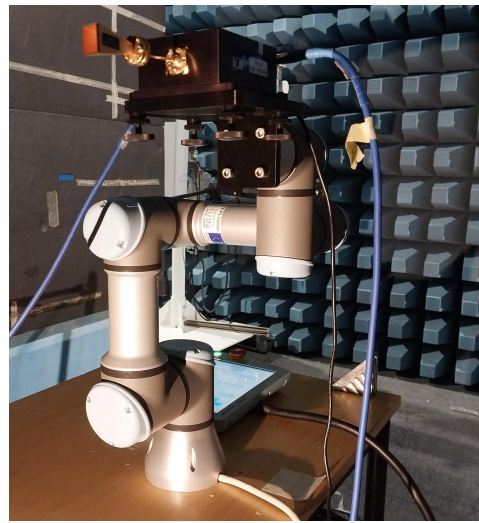


Fig. 3. Photo of the RX module with the antenna under test (AUT) mounted in the UR3 cobot arm.

extenders from Virginia Diodes Inc. which has a multiplication factor of 12, implying that the LO frequencies for both extenders are kept in the range of 9.17 GHz–14.17 GHz so as to cover the full range of carrier frequencies of 110–170 GHz. The transmitting (TX) and receiving (RX) antennas used in this setup are a pair of the PEWAN1028 type horn antenna from PASTERNAK having 25 dBi nominal gain. In order to perform the measurements of the E-plane cuts, a TW90D-02E waveguide twist component from Elmika were used at both the TX and RX ends. The TX module consisting of the TX frequency extender and horn antenna is mounted on a THORLABS L490/M lab jack and in this current setup has been placed on a movable trolley shelf. A custom 3-D printed holder plate having a thickness of 10 mm was manufactured to attach on the tool flange of the cobot using four 20 mm M6 screws. The RX module which consists of the RX frequency extender and antenna under test (AUT) is then mounted on top of this plate thereby making it an extension of the cobot.

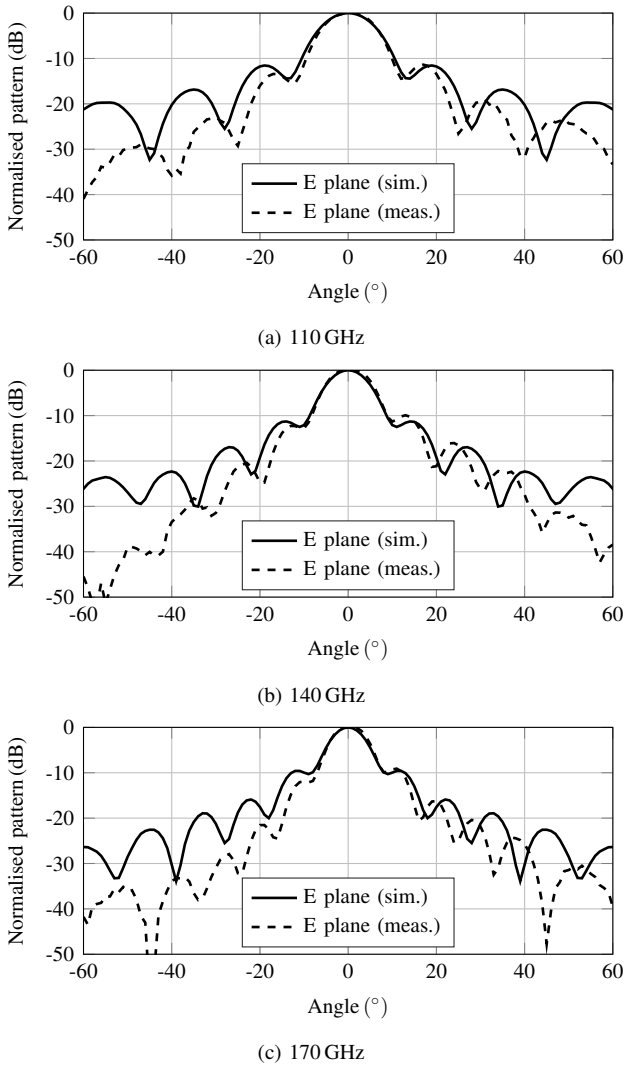


Fig. 4. Simulated and FF measured normalised *E*-plane co-polar patterns.

B. Measurement Setup

The measurement setup in the anechoic chamber is as depicted in Fig. 2, and Fig. 3 shows a close up of the UR3/CB3 cobot without absorbers. Also, a temporary enclosure treated with high frequency pyramid absorbers was built within the chamber in order to reduce the effects from reflections and scattering due to the measurement environment.

The RX module is mounted on the cobot with the measurement setup being configured to have the AUT as the receiving end. The reasoning behind having the RX frequency extender on the cobot is because there are fewer RF cable connections to it compared to the TX frequency extender which could limit the movement and induce more phase errors due to cable bending. In the current setup, cables are routed near the base of the workbench on which the cobot is mounted making sure there is enough strain relief and cable flexing has been minimized by using a SMA 90° male to female adapter on the RX frequency extender ports.

The TX module which was mounted on a trolley shelf has

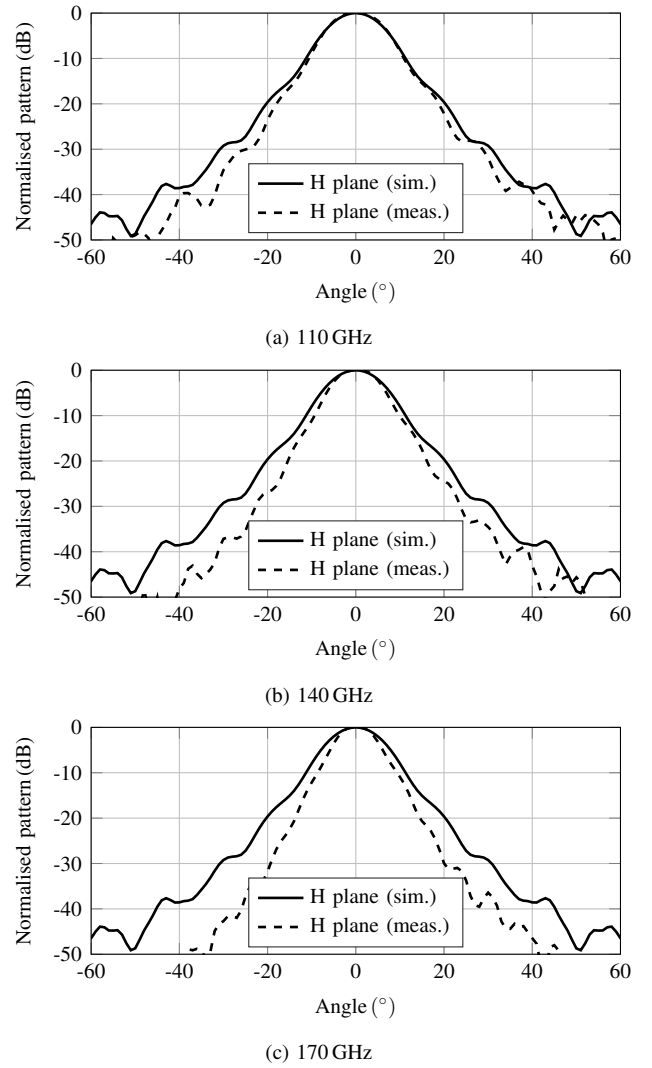


Fig. 5. Simulated and FF measured normalised *H*-plane co-polar patterns.

also been treated with flat sheet absorbers as seen in the setup in order to reduce the unwanted reflections. The TX antenna and AUT are then placed at an approximate aperture to aperture distance of 155 cm which ensures that they are in the far-field operation of each other at 110-170 GHz. The antennas are then aligned to each other at boresight direction with the help of an optical laser light.

C. Measurement Process

The required measurement parameters such as the pose coordinates, frequency range, resolution bandwidth, and power level of the network analyzer were defined in the Python code. After a measurement was initiated, the required parameters were sent over Ethernet to the cobot controller and the PNA.

In the current setup, point-to-point (PTP) measurements are carried out wherein the cobot is programmed to stop at each angular position defined in the coordinates and on reaching the specified pose it triggers the PNA to perform a measurement. Once the PNA has performed the measurement at the current

pose it sends a trigger back to the cobot to then proceed to the next pose coordinate. At each azimuth angle the data collected includes the pose coordinate, the joint angles of the cobot at that specific pose and the measured S-parameter data from the PNA. The code is developed such that all this information is appended in a buffer storage and only written on to the measurement data file once the trajectory is complete so as to not lose any measurement data due to synchronization issues from the triggering.

PTP measurements need more time compared to on-the-fly measurements where the cobot will traverse the trajectory with constant speed allowing for fast measurements with minimal vibrations due to deceleration. However, the measurements involved multiple frequencies within the sub-THz band, and thus PTP measurements was a better option comparatively as the cobot does not have to go through the entire trajectory multiple times for each frequency point thereby making the measurement accuracy a challenging task.

The IF bandwidth of the PNA-X was set as 10 kHz during the measurements as a bandwidth of 100 Hz and below was seen to cause a synchronization error between the cobot and the PNA-X. The standard operation waveguide attenuator on the RX extender was removed during the measurements, improving the dynamic range by about 25 dB.

Since the CW extender test ports are inherently vertically polarised, measurements are performed to obtain the H-plane cut and waveguide twists were then added at both the TX and RX extenders in order to capture the E-plane cut. This approach allowed us to use the same angular trajectory in the azimuth plane to obtain two cuts with minimal mechanical modification. Rotating the cobot arm by 90° would be an alternative approach but that would shift the alignment between the antennas and necessitate another alignment procedure hence increasing measurement uncertainties.

IV. MEASUREMENT RESULTS

A. EM Simulation Cuts and Far Field Measurements

Fig. 4 and Fig. 5 presents the comparison of simulated and measured FF co-polar E- and H-plane normalised patterns across the entire azimuth plane respectively. The figures show that a good agreement is obtained between the simulated and measured 2D-cut results at the main lobe. However, at the side lobes there is a slight deviation in the depth or direction of the nulls, especially at the negative angles because of a mechanical tilt in the waveguide twist due to manufacturing error.

B. E-Plane Comparison of EM Simulation, Planar Near Field and Far Field Measurements

Fig. 6 compares the co-polar E-plane patterns around the main beam from two different measurement techniques with the simulations. A detailed description of the planar NF measurement technique has been previously presented in [9]. A good matching between the two measurement techniques compared to the simulation result in terms of the main lobe and first three side-lobes can be observed. The slight deviations in the NF patterns are due to the interpolation of data beyond the

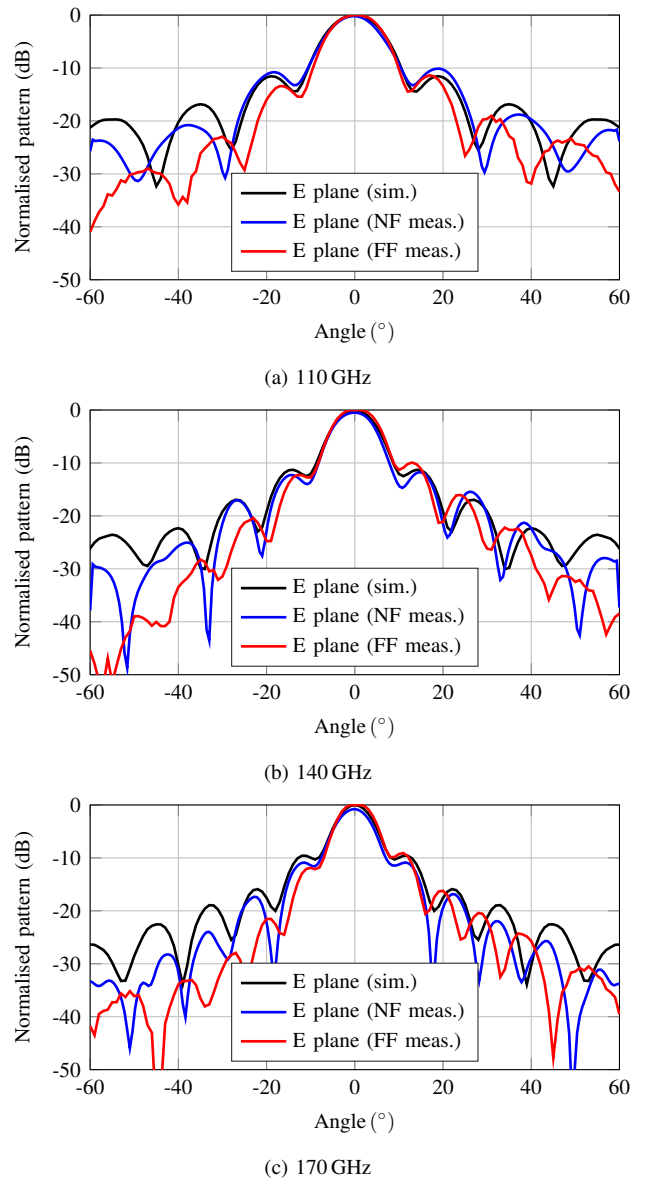


Fig. 6. Simulated and measured (NF and FF) normalised E-plane co-polar patterns.

TABLE I
MEASUREMENT DISTANCES

Frequency	d_{NF}	d_{FF}
110 GHz	4.1 cm	≥ 37.8 cm
140 GHz	4.6 cm	≥ 48.1 cm
170 GHz	5.0 cm	≥ 58.4 cm

scan range of the measurement system while the deviations in the FF patterns are due to the mechanical tilt in the waveguide twist. Also, at larger angles we notice slight fluctuations in the FF measured patterns originating from the scattering effects of the measurement environment.

C. Distance Analysis of Far Field Measurements

This analysis is carried out to verify experimentally the FF conditions in a direct FF measurement setup. In [10], it has

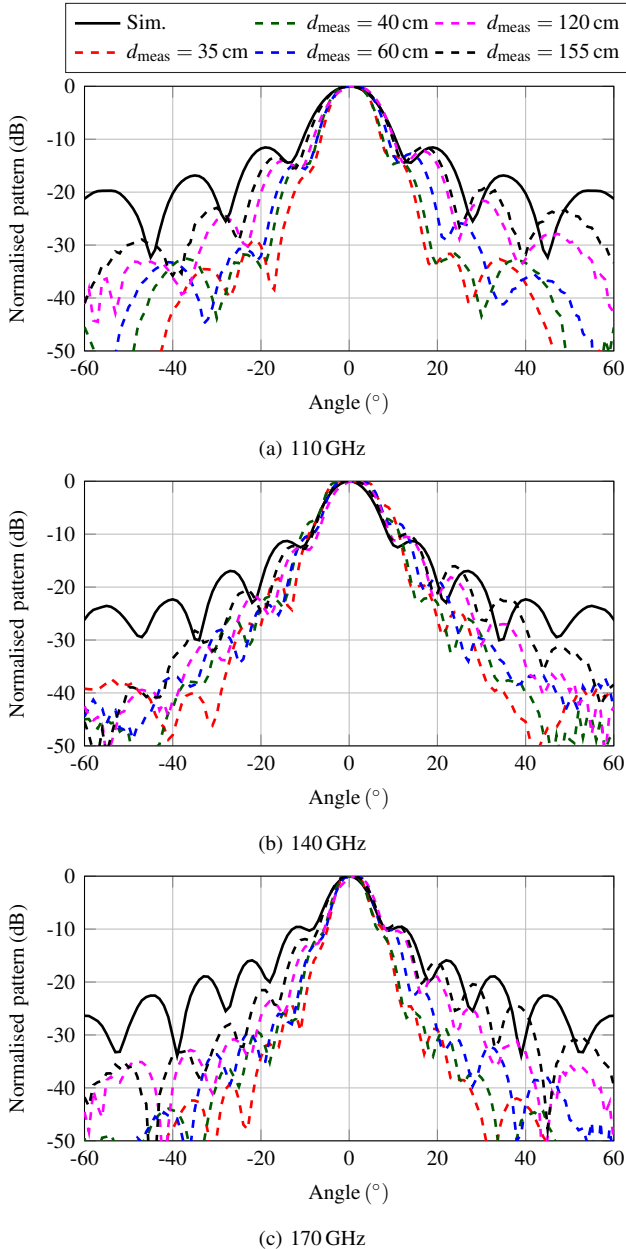


Fig. 7. Simulated and FF measured normalised E -plane co-polar patterns at different distances. All figures share the same legends.

been shown through measurements that acceptable results can still be achieved below the Fraunhofer distance at mm-wave frequencies of 27 GHz and 38 GHz. In this paper we have extended this study to the sub-THz band of 110-170 GHz. A description of the theoretical NF and FF distances of the AUT having largest dimension of 22.68 mm used in the analysis of this work is given in Table I. FF measurements were carried out at approximate distances strategically in the NF of all frequencies ($d_{\text{meas}} = 35$ cm), then at the edge of the FF for 110 GHz ($d_{\text{meas}} = 40$ cm), followed by the edge of the FF of all frequencies ($d_{\text{meas}} = 60$ cm) and finally at twice the theoretical FF ($d_{\text{meas}} = 120$ cm). From the results in Fig. 7, we can infer that the correlation of the main lobe and first two side-lobes

are possible at all of the measured distances. As the distance increases, the patterns will match better to the simulation result as expected. However, if deviations are in the acceptable range for a measurement case scenario, measurement distances can be substantially reduced.

V. CONCLUSION

This paper has presented a detailed description of an initial stage antenna measurement setup that is based on a cobot model from Universal Robots offering flexibility in RF OTA measurements. FF measured results in the E - and H -plane co-polar radiation patterns show a decent matching with simulations when considering the sparse measurement trajectory applied within the measurement system. Further, comparative analysis using the NF measurement technique has been presented to validate the robotic measurement system, albeit further improvements are to be carried out.

ACKNOWLEDGMENT

This research was supported by Business Finland RF Sampo project under Grant 2993/31/2021, in part 6G-XR project funded from the SNS JU under the EU's Horizon research and innovation programme (Grant Number: 101096838), and in part by 6G Flagship (Grant Number 369116) funded by the Research Council of Finland. Keysight Technologies, Inc. has supported the research with measurement equipment donation. Simulation results have been obtained using computational resources from CSC – IT Centre for Science, Finland.

REFERENCES

- [1] A. Pärssinen *et al.*, "White paper on RF enabling 6G – opportunities and challenges from technology to spectrum," University of Oulu, 2020, White paper, (6G Research Visions, No. 13).
- [2] C. A. Balanis, *Antenna Theory: Analysis and Design*, 3rd ed. Hoboken, NJ: John Wiley, 2005.
- [3] A. Yaghjian, "An overview of near-field antenna measurements," *IEEE Trans. Antennas Propag.*, vol. 34, no. 1, pp. 30–45, Jan. 1986.
- [4] J. A. Gordon *et al.*, "Millimeter-wave near-field measurements using coordinated robotics," *IEEE Trans. Antennas Propag.*, vol. 63, no. 12, pp. 5351–5362, Dec. 2015.
- [5] D. M. Lewis, J. Bommer, G. E. Hindman, and S. F. Gregson, "Traditional to modern antenna test environments: The impact of robotics and computational electromagnetic simulation on modern antenna measurements," in *2021 15th Eur. Conf. Antennas Propag. (EuCAP)*, Düsseldorf, Germany, Mar. 2021, pp. 1–5.
- [6] X. Liu, C. Huang, and Y. Cheng, "Antenna planar near-field measurement system using robotics," in *2021 13th Global Symp. Mm-Waves & THz (GSMM)*, Nanjing, China, May 2021, pp. 1–3.
- [7] M. Meng *et al.*, "Robotic radiation pattern measurement system for 6–110 GHz based in both near field and far field," in *2023 IEEE Int. Opport. Res. Schol. Symp. (ORSS)*, Atlanta, GA, USA, Apr.-June 2023, pp. 11–15.
- [8] M. Hitzler, S. Bader, and C. Waldschmidt, "Key aspects of robot based antenna measurements at millimeter wave frequencies," in *The 8th Eur. Conf. Antennas Propag. (EuCAP 2014)*, The Hague, The Netherlands, Apr. 2014, pp. 392–396.
- [9] A. Husein *et al.*, "Characterisation of a D-band horn antenna: Comparison of near-field and OTA measurements," in *2024 18th Eur. Conf. Antennas Propag. (EuCAP)*, Glasgow, UK, Mar. 2024, pp. 1–5.
- [10] J. Fromme *et al.*, "On over-the-air far-field measurements below Fraunhofer distance," in *2021 97th ARFTG Microw. Meas. Conf. (ARFTG)*, Atlanta, GA, USA, June 2021, pp. 1–4.